Available online at www.sciencedirect.com
ScienceDirect
Carbohydrate Research 343 (2008) 73–80
Carbohydrate RESEARCH

# Cellulose synthesized by *Acetobacter xylinum* in the presence of multi-walled carbon nanotubes

Zhiyong Yan, Shiyan Chen, Huaping Wang,* Biao Wang, Chaosheng Wang and Jianming Jiang

*State Key Laboratory for Modification of Chemical Fibers and Polymer Materials, Donghua University, Shanghai 201620, PR China*

Received 14 September 2007; received in revised form 19 October 2007; accepted 24 October 2007
Available online 1 November 2007

**Abstract**—The structure of bacterial cellulose is affected by the bacterial strain used, culture media and cultivation conditions. In this study, acid-treated multi-walled carbon nanotubes (MWNTs) were added into a static culture medium and their effect on bacterial cellulose structure was studied by scanning electron microscopy (SEM), atomic force microscopy (AFM), Fourier transform infrared spectroscopy (FT-IR), CP/MAS $^{13}C$ NMR and X-ray diffractometry. The bacterial cellulose ribbons and the MWNTs interwound and formed a three-dimensional network architecture. Band-like assemblies with sharp bends and rigidity were also produced in the presence of MWNTs. The intermolecular hydrogen bonds in bacterial cellulose produced in the presence of MWNTs were weakened. The crystal structure, cellulose $I_\alpha$ content, crystallinity index (CrI) and crystallite size all changed. The results may suggest that the acid-treated MWNTs containing hydroxyl groups interact with the sub-elementary bacterial cellulose fibrils, subsequently interfering with the aggregation and crystallization.


*Keywords:* Bacterial cellulose; MWNTs; Cellulose $I_\alpha$; Cellulose $I_\beta$; Crystallinity index

## 1. Introduction

Bacterial cellulose (BC) can be synthesized as microfibrils by aerobic Gram-negative, acetic acid bacteria *Acetobacter xylinum* (reclassified as *Gluconacetobacter xylinus*) using linear terminal enzyme complexes.[1] It has been suggested that the alteration of chemical or biochemical conditions during the biosynthesis could alter the high order structure of cellulose assemblies. For example, cell division can be depressed by adding antibiotics to the incubation medium[2] resulting in broader microfibrils than those generated under normal conditions. It was postulated that the growth rate of cell division may be connected to the bacterial motion.[3] The motion of a single bacterium incubated in a viscous medium[4] or at low temperature[5,6] was changed, leading to the alteration of the morphology and crystal structure, which may be attributed to the changes of the number and array of terminal complex subunits of the bacterium.

The biosynthesis of BC involves polymerization and crystallization processes.[7] Although crystallization occurs soon after the glucan chains have been extruded from the cell, it does not occur instantaneously. Based on the two-step model proposed by Cousins and Brown,[8,9] it was assumed that the factors that affect either step will influence the final structure of the BC. Experimentally, many studies have focused on the modification of the crystallization process by adding water-soluble agents into the culture medium. Modification of BC by structurally related molecules was first studied with carboxymethyl cellulose (CMC), which was found to delay the aggregation of cellulose microfibrils.[10] Calcofluor white added to the culture medium prevented the assembly of individual microfibrils and prohibited the crystallization through binding with hydroxyl

* Corresponding author. Tel.: +86 21 67792958; fax: +86 21 67792726; e-mail: wanghp@dhu.edu.cn

0008-6215/$ - see front matter © 2007 Published by Elsevier Ltd.
doi:10.1016/j.carres.2007.10.024

groups in straight chain polysaccharides.[7,11] It had been found that the proportion of cellulose $I_\alpha/I_\beta$ was decreased in the presence of water-soluble hemicellulose.[12] A similar conclusion could be drawn when xyloglucan was added to the incubation medium.[13,14] Xylan in the culture medium can stick on the surface of individual microfibrils inhibiting them from forming ribbons and decreasing the crystal size and the ratio of cellulose $I_\alpha$.[15,16] Therefore, it can be safely concluded that adding water-soluble agents into the culture medium can affect the assembly and crystallization of glucan chains.

Aside from water-soluble agents, the effect of some water-insoluble solid particles added to the culture medium was also studied.[17] Some solid particles can be trapped to form a composite material depending on the shape and dimension of the particles. Only the smallest particles were incorporated rapidly into the cellulose film and the largest ones were barely incorporated. However, there are few studies on cellulose biosynthesis in the presence of water-insoluble nanofibers with a high aspect ratio.

Multi-walled carbon nanotubes (MWNTs) are nearly one-dimensional nanomaterials with a high aspect ratio, as well as superior mechanical and electrical properties.[18–21] The MWNTs and bacterial cellulose fibrils, which are nanofibers, could be used as biomaterials such as artificial muscles or artificial blood vessels.[22,23] It can be expected that the MWNTs/BC composites will be used widely as biomaterials. An attractive method for preparing such composites is in situ biosynthesis in the presence of MWNTs in the culture medium. To improve physicochemical compatibility between MWNTs and BC, it is necessary to modify MWNTs by a chemical treatment using concentrated nitric acid and sulfuric acid to obtain better dispersion and hydrophilicity of the individual fibrils.[24] As a result, the broken C–C bonds at the tube ends were capped by various oxygen-containing functional groups, such as –COOH, –OH and –C=O.

In this study, the acid-treated MWNTs were added to the culture medium containing *A. xylinum* 1.1812 strain, and their effect on the structure of cellulose microfibrils was investigated by SEM, AFM, FT-IR, CP/MAS $^{13}C$ NMR and X-ray diffractometry.

## 2. Materials and methods

### 2.1. Functionalization of MWNTs

The MWNTs (purity, >97%) were kindly provided by Tsinghua-Nafine Nano-Powder Commercialization Engineering Center, Beijing, China. Their outer diameters are 20–40 nm and their lengths are about 10–50 μm. MWNTs (400 mg) was suspended in 400 mL of a mixture of concentrated nitric acid (68%) and sulfuric acid (98%) (1:3 in volume ratio) and heated at reflux at 80 °C for 10 h. Then, the samples were filtered with PTFE (poly-(tetrafluoroethylene)) membrane with the pore size of 0.1 μm in deionized water and ultrasonicated in a 120 W and 59 kHz ultrasonic bath for 30 min prior to use.

### 2.2. BC culture media and condition

*A. xylinum* 1.1812 strain was kindly provided by Institute of Microbiology, Chinese Academy of Science. Two types of culture media were used: the Hestrin–Schramm culture medium (HS) (2.5% w/v D-glucose, 0.5% w/v peptone, 0.5% w/v yeast extract, 0.115% w/v citric acid and 0.25% w/v disodium hydrogen phosphate) and MWNT-HS medium (in the presence of final 0.005% w/v MWNTs in HS medium). These culture media were sterilized at 121 °C in autoclave for 30 min by autoclaving and poured into Erlenmayer flasks. These cultures were incubated statically at 28 °C at pH 6.0 for two weeks. The harvested BC membranes were boiled in 1% sodium hydroxide solution for 30 min, then rinsed for three days to pH 7 in deionized water and dried in air at room temperature.

### 2.3. SEM and AFM observation

The samples dried in air were coated with gold palladium by cathodic spreading in a Polaron E 5100 coater and examined with a JSM-5600LV (JEOL, Japan) SEM operated at an accelerating voltage of 15 kV.

The AFM used to image the membrane surfaces was a multimode scanning probe microscope with a NanoScope IV controller, supplied by Digital Instruments (Santa Barbara, CA). Small pieces were cut from each membrane, glued onto metal disks and attached to a magnetic sample holder located on top of the scanner tube. The membrane surface was scanned in the tapping mode. All the AFM images were undertaken at 25 °C.

### 2.4. FT-IR spectroscopy

The acid-treated MWNTs were well mixed with potassium bromide (KBr) powder, dried at 50 °C under vacuum and pressed into a small tablet. The BC membrane with or without MWNTs was dried at 40 °C under vacuum. FT-IR spectra were recorded on a Nicolet model 6000C equipped with a MCT detector in the absorption mode with a resolution of 4 $cm^{-1}$ in the range of 4000–400 $cm^{-1}$. The mass fraction of cellulose $I_\alpha$, $f_\alpha^{IR}$ was estimated from the Eq. 1,[25]

$$f_\alpha^{IR} = \frac{A_{750}}{A_{750} + kA_{710}} \quad (1)$$

where $A_x$ is the integrated absorption at the corresponding wavenumber and $k$ is the constant ($k = 0.16$).

### 2.5. X-ray diffractometry

The air-dried thin-membranes were used as the sample. X-ray diffractometry in reflection mode was carried out in reflection mode ($2\theta = 5$–$60°$) using a D/Max-2550 PC with Cu K$\alpha$ radiation generated at 40 kV and 30 mA. The diffraction profile was processed by computer-aided fitting analysis and transformed to basic crystallographic features: d-spacings of equatorial lattice planes.

### 2.6. CP/MAS $^{13}$C NMR spectroscopy

The membranes prepared for NMR measurements were mechanically disintegrated into smaller fragments, which were packed into a MAS rotor with an O-ring seal after full hydration. CP/MAS $^{13}$C NMR measurements were performed with an Avance 400 (Bruker Co. Ltd, Switzerland) spectrometer with a static magnetic field of 9.4 T. $^{1}$H and $^{13}$C radiofrequency field strengths ($\gamma B_1/2\pi$) were 4.2 μs for both CP and dipolar decoupling processes. The MAS rate was set to 5.6–5.8 kHz, and the contact time for the CP process was 1.0 ms. The $^{13}$C chemical shift relative to tetramethylsilane ($(CH_3)_4Si$) was calibrated using the $CH_3$ carbon line at 17.36 ppm of hexamethylbenzene crystals as an external reference. Line shape analysis was carried out for C4 resonance using the least-squares fitting algorithm and $I_\alpha$ fraction: $f_\alpha$ was calculated from the Eq. 2,[26]

$$f_\alpha^{\mathrm{NMR}} = 0.5 + f_{90.3} - f_{88.6} \quad (2)$$

where $f_x$ denotes the integrated fraction at the corresponding ppm.

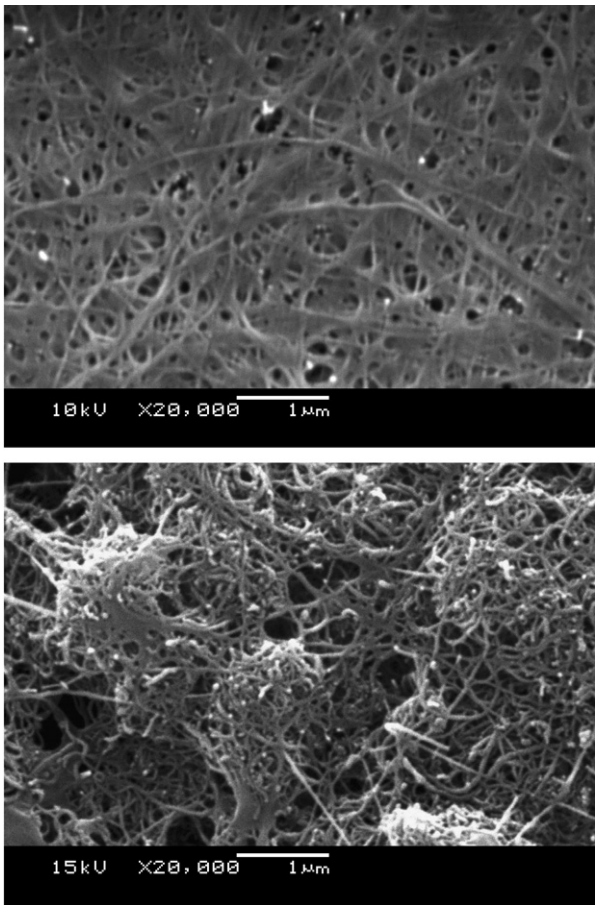


**Figure 1.** SEM images of BC membrane (a) and BC interwound with MWNTs (b).

## 3. Results and discussion

### 3.1. Morphology of BC produced in the absence and presence of MWNTs (MWNT-BC)

Figure 1a shows the scanning electron micrographs of the BC membrane incubated in the HS medium. The BC ribbons produced in the HS medium are about 40–60 nm wide and construct the pore-like reticulated structure. Figure 1b shows the BC and MWNTs network produced in the MWNT-HS medium. The bright regions in Figure 1b are attributed to the MWNTs. The MWNTs are apparently incorporated into the BC microfibril network. The MWNTs and BC microfibrils curl up and interwind into a crosslinked three-dimensional porous network. The two kinds of nanofibers are 40–60 nm wide, and it is difficult to discern them in the network (Fig. 1b). In contrast, the ribbons in HS medium appear more highly extended, assembling into a layer-by-layer membrane (Fig. 1a).

The typical structure of cellulose produced by *A. xylinum* in HS medium was a ribbon-like assembly.[27] However, the dense band-like assembly of BC could be produced at 4 °C.[6] *A. xylinum* 1.1812 incubated in MWNT-HS medium can also produce the band-like cellulose assemblies as shown in Figure 2a. The bands are apparently deformed, bent sharply and appear flatter, wider and more rigid than those ribbons. The widths of the bands change in the range of 400–900 nm. However, the BC ribbons (Fig. 2b) produced in the HS medium are almost circular, highly extended and only 40–60 nm wide. It implies that the acid-treated MWNTs may influence the ribbon formation. There is a strong relationship between the synthesizing terminal complexes (TCs) in the bacteria and the dimensions of cellulose microfibril.[9] The physical constraints on cell movement, such as solidified HS or viscous medium and the spatial obstacle, were supposed to be very important for the changes of cellulose structure. Hirai and his co-workers proposed that the specific movements of the cells may be hindered, and then the performance of enzyme systems in a synthesizing terminal complex subunit may be depressed.[6] Ross et al. proposed that the activity of TCs in the bacterium was depressed and the array of the TCs subunits could be

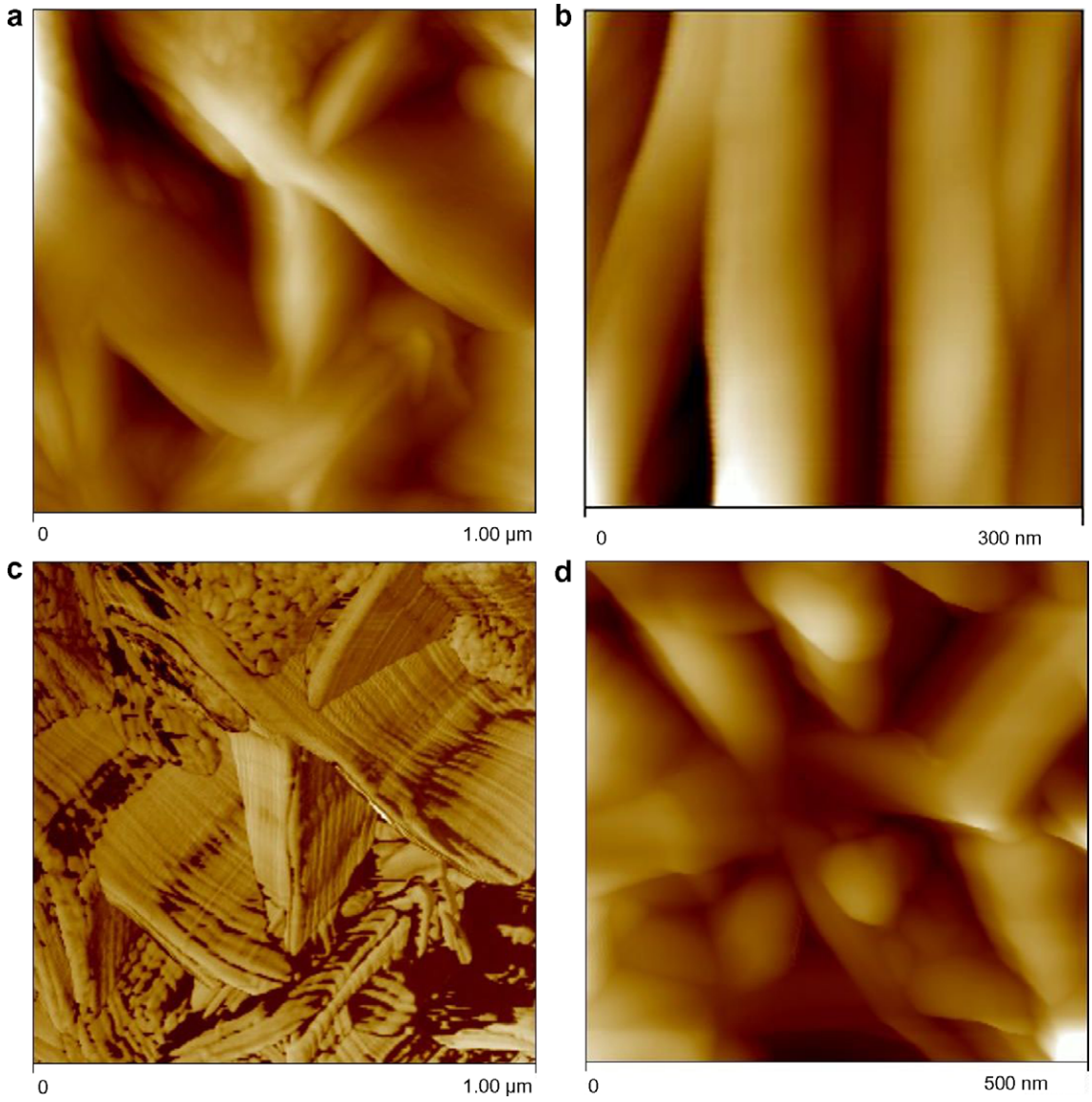


**Figure 2.** (a) AFM height image of the MWNT-BC; (b) AFM image of the BC ribbons; (c) AFM phase image of the MWNT-BC; (d) AFM image of MWNTs embedded into the BC bands network.

changed.[28] Shibazaki et al. suggested that the band-like cellulose could be induced by a low mobility of cells in the high viscous culture medium due to physical constraints.[4] In this study, the acid-treated MWNTs are dispersed uniformly in the culture medium and form a dense carbon nanotube network. The bacterial cells were about 1 μm wide and over 4 μm long,[2] bigger than the dimension of MWNTs. It may be that the bacterial cells could not move freely at the first stage because of the spatial obstacle of MWNTs and the activity of TCs is depressed, resulting in band-like assemblies.[3]

Figure 2c shows that each band is composed of scores of 1.5–3 nm wide sub-elementary fibrils arranged side by side. The MWNTs delay the sub-elementary fibrils aggregating into ribbons according to Tokoh et al.[29] It may be that the –OH groups in the acid-treated MWNTs interact with the –OH groups in the cellulose microfibrils and weaken the interaction between the sub-elementary fibrils, inhibiting their aggregation.

Figure 2d shows that an individual multi-walled carbon nanotube is embedded into the BC bands network. The individual carbon nanotube is enclosed by the BC bands, which indicate that the acid-treated MWNTs are separately dispersed in the medium and interact strongly with the BC.

### 3.2. FT-IR spectroscopy analysis

Figure 3 shows the FT-IR spectrum of the MWNTs treated by the concentrated acid mixture. The peaks at 1728 and 1586 $cm^{-1}$ indicate that carboxylic acid groups and carboxylate groups exist on the surface.[30] The

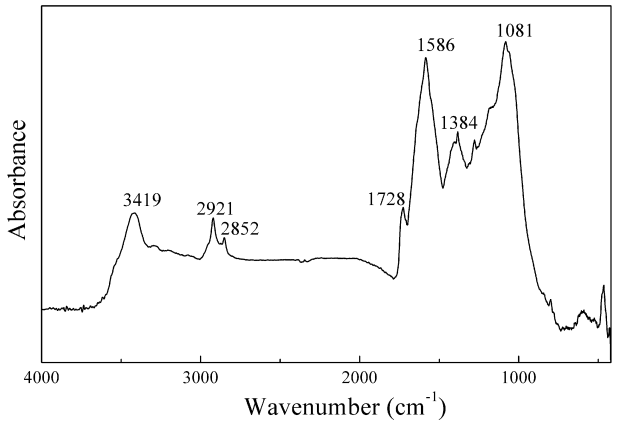


**Figure 3.** The FT-IR spectrum of the acid-treated MWNTs.

bands of 2852 and 2921 $cm^{-1}$ are attributed to $CH_2$ stretching. The peak at 1081 $cm^{-1}$ could be associated with ether C–O–C functionalities.[24] The band at 3419 $cm^{-1}$ is attributed to the presence of hydroxyl groups (–OH). All these peaks indicate the oxidation of MWNTs by concentrated $H_2SO_4/HNO_3$.

Figures 4a and b show the FT-IR spectra of BC and MWNT-BC, the spectrum a and spectrum b, respectively. The absorption band near 750 $cm^{-1}$ is attributed to the contribution of cellulose $I_\alpha$, whereas 710 $cm^{-1}$ corresponds to the contribution from cellulose $I_\beta$.[31–33] The intensity of the peak near 710 $cm^{-1}$ is lower relative to 750 $cm^{-1}$ in spectrum a, on the contrary, the intensity of the peak near 710 $cm^{-1}$ is higher relative to 750 $cm^{-1}$ in spectrum b (Fig. 4b). It shows that the cellulose $I_\alpha$ content in BC is higher than that in MWNT-BC. To determinate the cellulose $I_\alpha$ content quantitatively, the absorption bands at 750 and 710 $cm^{-1}$ were deconvoluted by using Lorenzian curve fitting analysis on the original spectra. The mass fraction of cellulose $I_\alpha$ could be calculated according to Eq. 1. The cellulose $I_\alpha$ content for BC and MWNT-BC is 76.3% and 66.7%, respectively.

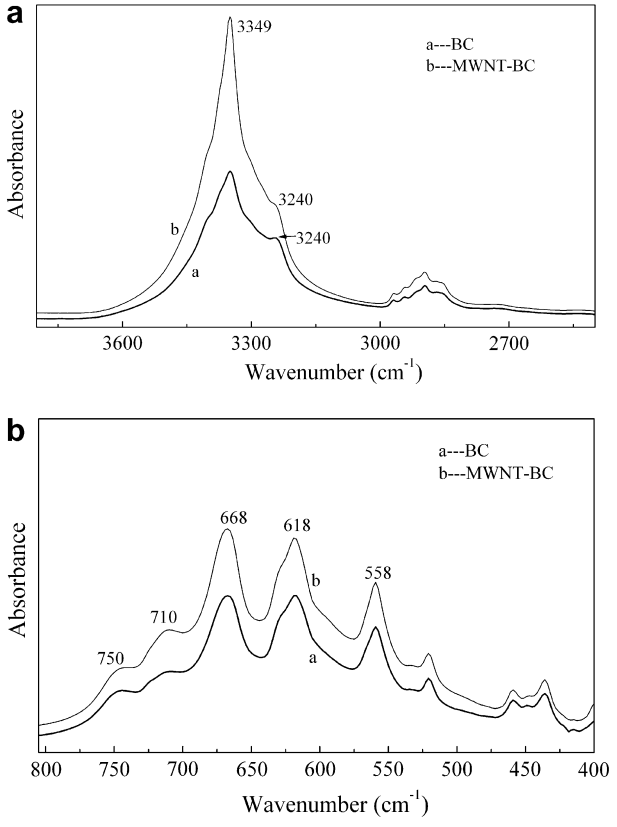


**Figure 4.** FT-IR spectra of (a) 3800–2500 $cm^{-1}$ and (b) 805–400 $cm^{-1}$ of BC (spectrum a) and MWNT-BC (spectrum b).

The bands in the region 3600–3000 $cm^{-1}$ (Fig. 4a) correspond to the O–H stretching frequencies of cellulose.[34] It is particularly useful for elucidating hydrogen-bonding patterns because, in favourable cases, each distinct hydroxyl group gives a single stretching band at a frequency that decreases with increasing strength of hydrogen bonding.[35] In the cellulose crystals, the conformation of the cellulose chains, as well as their strong packing depends on intermolecular and intramolecular hydrogen bonds. The intramolecular hydrogen bonds for 2-OH···O-6 and 3-O···HO-5, and the intermolecular hydrogen bonds for 6-O···HO-3 in cellulose I appear at 3455–3410, 3375–3340 and 3310–3230 $cm^{-1}$, respectively, along with the valence vibration of H-bonded OH groups at 3570–3450 $cm^{-1}$.[36] In Figure 4a, there is a significant peak at 3240 $cm^{-1}$ in spectrum a, which is attributed to the cellulose $I_\alpha$.[33] It implies that the cellulose $I_\alpha$ content in BC is higher, which agrees with the data for $f_\alpha^{IR}$. The intensity ratio of the band at 3240–3349 $cm^{-1}$ in spectrum b is lower than that in spectrum a, which indicates that the intermolecular hydrogen bonds in MWNT-BC are weaker relative to those in BC. That is to say that the intermolecular hydrogen bonds in MWNT-BC are weakened compared with those in BC.

The crystallinity index ($CrI^{IR}$) of cellulose could be evaluated by the intensity ratio $H_{1429}/H_{897}$ between FT-IR absorptions at 1429 and 897 $cm^{-1}$.[37] The absorbance at 1429 and 897 $cm^{-1}$, which are assigned to $CH_2$ bending mode and deformation of anomeric CH, respectively,[38] are sensitive to the amount of crystalline versus amorphous structure in the cellulose. The values of $CrI^{IR}$ for BC and MWNT-BC are 9.9 and 7.6, respectively. The $CrI^{IR}$ for BC is higher than that for MWNT-BC, implying that the MWNTs influence the aggregation and crystallization of BC microfibrils.

### 3.3. CP/MAS solid $^{13}C$ NMR spectra

CP/MAS solid $^{13}C$ NMR spectra are a useful tool to characterize cellulose allomorphs. Figure 5 shows the CP/MAS solid $^{13}C$ NMR spectra of BC (spectrum a) and MWNT-BC (spectrum b). The chemical shift signals

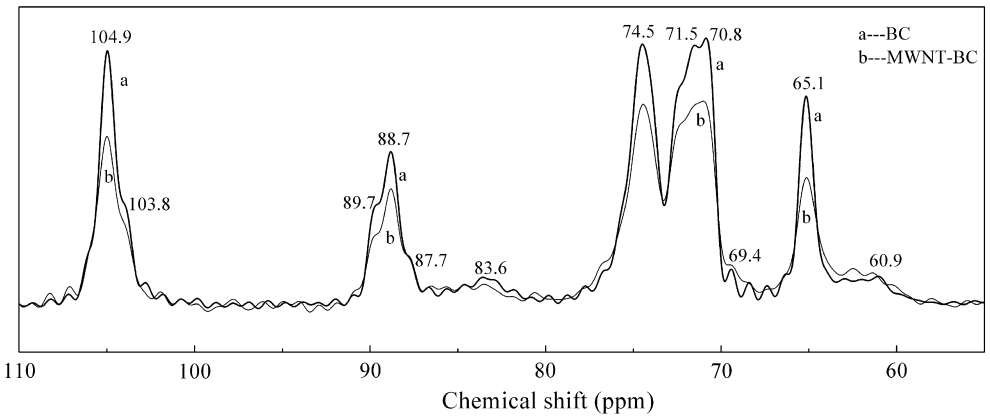


**Figure 5.** Comparison of the CP/MAS $^{13}C$ NMR of BC (spectrum a) and MWNT-BC (spectrum b).

at 89.7, 88.7, and 87.7 ppm are due to the crystalline cellulose, while the signal at 83.6 ppm is indicative of the amorphous cellulose, which suggests that they are the typical cellulose I.[39–41] The C-1 resonance line of the spectrum a of BC is a triplet, which is composed of an enhanced central line and a considerably smaller doublet beside the central line. It indicates that cellulose $I_\alpha$ is dominant in BC.[26] In the case of MWNT-BC, there is an obvious decrease in the relative intensities of the corresponding resonance lines for the C-4 and C-1 triplets, suggesting the decrease in the mass fraction of cellulose $I_\alpha$. It was assumed that the C-4 triplet was composed of the linear combination of the spectra of cellulose $I_\alpha$ and $I_\beta$.[40] The mass fractions of the respective allomorphs are determined from their contribution to the C-4 triplet.[41] To calculate the precise content of cellulose $I_\alpha$ in the cellulose, we deconvoluted the C-4 signal to obtain the respective subspectra of cellulose $I_\alpha$ and $I_\beta$ phases from the original spectrum.[42] Therefore, the spectra of C-4 region were assigned to three Lorentzian lines for the signals from $I_\alpha$, $I_{(\alpha+\beta)}$ and $I_\beta$. The mass fraction of cellulose $I_\alpha$, $f_\alpha^{NMR}$, is determined by the Eq. 2. The values of $f_\alpha^{NMR}$ for BC and MWNT-BC are 86.7% and 79.6%, respectively. The mass fraction of cellulose $I_\alpha$ in BC is higher than that in MWNT-BC, as $f_\alpha^{IR}$ shows. The results are consistent with the addition of CMC, xylan and mannan in the culture medium.[13,15,16,29] Wada et al. proposed that the cellulose $I_\alpha$ and $I_\beta$ had preference for linear-type and rosette-type TCs, respectively.[43] It may be that the spatial obstacle of MWNTs in the medium depresses the activity of TCs and changes the array of TCs subunits, resulting in more cellulose $I_\beta$.

### 3.4. X-ray diffractometry

Figure 6 shows the diffraction patterns of acid-treated MWNTs, BC and MWNT-BC. The pattern for acid-treated MWNTs exhibits two main peaks at 25.82°

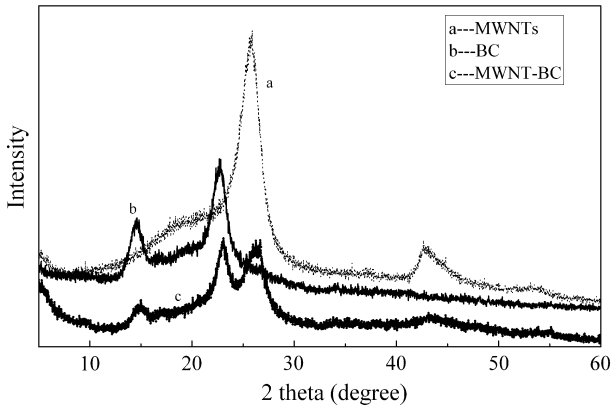


**Figure 6.** Wide-angle X-ray diffractograms of MWNTs, BC and MWNT-BC.

and 42.72°, corresponding to the (002) and (100) reflection, respectively.[44] The BC crystallites show main peaks at 14.53° and 22.71°, corresponding to the crystallographic plane of (101) and (002), respectively. These data indicate that the BC sample is the typical crystalline forms of cellulose I.[36,45] The MWNT-BC crystallites show the main peaks for cellulose I at 14.88° and 23.01°, and the peaks for MWNTs at 26.48° and 43.20°. It indicates that a large number of MWNTs are embedded into the BC network as shown in Figure 1b. The positions of the corresponding diffraction peaks shift to wider angles in the MWNT-BC. Their interplanar distances of the crystallites (d-spacings) could be calculated with Bragg's law. The d-spacings of (101) and (002) planes for BC are 6.09 and 3.91 Å, respectively, while those for MWNT-BC are 5.95 and 3.86 Å, respectively. The d-spacing value of (101) plane decreases by the addition of xylan or mannan, and that of the (002) plane increases.[16] The d-spacings of (101) and (002) plane for MWNT-BC both decrease, which implies that the acid-treated MWNTs interfere with the crystallization of nascent cellulose microfibrils at the early stage, however, hemicelluloses do not influence the early stage of cellulose assembly.[15]

The crystallite sizes for cellulose can be calculated using Scherrer's formula. The crystallite size of (002) plane decreases from 5.64 nm for BC to 5.46 nm for MWNT-BC, indicating the existence of smaller size crystallite in MWNT-BC. Similar results were obtained by adding xylan, glucomannan and mannan into the culture medium.[15,16,29] According to the three successive stages of cellulose assembly,[29] the reduction in crystallite size caused by the addition of MWNTs to the medium indicates that crystallization is not complete in the second stage. It may be that the acid-treated MWNTs strongly interact with sub-elementary fibrils, weaken the intermolecular hydrogen bonds and interfere with the aggregation and crystallization, while the processes of orientation and crystallization in cellulose depended largely on the intermolecular hydrogen bonds formed by the hydroxyl groups.

The acid-treated MWNTs with ─OH groups were dispersed uniformly in the HS medium. The BC ribbons interwound with the MWNTs and formed the three-dimensional network. Moreover, the band-like assemblies consisting of scores of 1.5–3 nm wide sub-elementary fibrils were also produced in the presence of MWNTs. It may be that the spatial obstacle of MWNTs in the medium depresses the activity of TCs and changes the array of the TCs subunits at the first stage of cultivation, which also decreases the cellulose $I_\alpha$ content in MWNT-BC. The FT-IR spectrum shows that the intermolecular hydrogen bonds in MWNT-BC are weakened. It may be that the MWNTs containing –OH groups could interact with the –OH groups in sub-elementary fibrils and further interfere with the aggregation and crystallization of sub-elementary fibrils, resulting in the incomplete crystallites. As a result, the d-spacings, crystallite sizes and CrI are decreased by adding MWNTs into the medium from XRD and CP/MAS NMR analyses. Similar results were obtained by adding Calcofluor White, CMC, XG, xylan and mannan into the culture medium.[11,13,15,16,29]

## Acknowledgements

This work was financially supported by the 111 project (B07024), School Fund and New Century Excellent Talents in University (NCET-05-0420).

## References

1. Yamada, Y.; Hoshino, K.; Ishikawa, T. *Biosci. Biotechnol. Biochem.* **1997**, *61*, 1244–1251.
2. Yamanaka, S.; Ishihara, M.; Sugiyama, J. *Cellulose* **2000**, *7*, 213–225.
3. Hesse, S.; Kondo, T. *Carbohydr. Polym.* **2005**, *60*, 457–465.
4. Shibazaki, H.; Saito, M.; Kuga, S.; Okano, T. *Cellulose* **1998**, *5*, 165–173.
5. Hirai, A.; Tsuji, M.; Horii, F. *Cellulose* **1997**, *4*, 239–245.
6. Hirai, A.; Tsuji, M.; Horii, F. *Cellulose* **2002**, *9*, 105–113.
7. Benziman, M.; Haigler, C. H.; Brown, R. M., Jr.; White, A. R.; Cooper, K. M. *Proc. Natl. Acad. Sci. U.S.A.* **1980**, *77*, 6678–6682.
8. Cousins, S. K.; Brown, R. M., Jr. *Polymer* **1995**, *36*, 3885–3888.
9. Inder, M. S.; Brown, R. M., Jr. *Ann. Bot.* **2005**, *96*, 9–21.
10. Ben-Hayyim, G.; Ohad, I. *J. Cell Biol.* **1965**, *25*, 191–207.
11. Haigler, C. H.; Brown, R. M., Jr.; Benziman, M. *Science* **1980**, *210*, 903–906.
12. Whitney, S. E. C.; Brigham, J. E.; Darke, A. H. *Plant J.* **1995**, *8*, 491–504.
13. Yamamoto, H.; Horii, F.; Hirai, A. *Cellulose* **1996**, *3*, 229–242.
14. Hirai, A.; Tsuji, M.; Yamamoto, H.; Horii, F. *Cellulose* **1998**, *5*, 201–213.
15. Tokoh, C.; Takabe, K.; Sugiyama, J.; Fujita, M. *Cellulose* **2002**, *9*, 65–74.
16. Tokoh, C.; Takabe, K.; Sugiyama, J.; Fujita, M. *Cellulose* **2002**, *9*, 351–360.
17. Serafica, G.; Mormino, R.; Bungay, H. *Appl. Microbiol. Biot.* **2002**, *58*, 756–760.
18. Iijima, S. *Nature* **1991**, *354*, 56–58.
19. Biercuk, M. J.; Llaguno, M. C.; Radosvljevic, M.; Hyun, J. K.; Johnson, A. T. *Appl. Phys. Lett.* **2002**, *80*, 15.
20. Showkat, A. M.; Lee, K. P.; Gopalan, A. I.; Kim, S. H.; Choi, S. H.; Sohn, S. H. *J. Appl. Polym. Sci.* **2006**, *101*, 3721–3729.
21. Avouris, P. *Chem. Phys.* **2002**, *281*, 429–445.
22. Vohrer, U.; Kolaric, I.; Haque, M. H.; Roth, S.; Detlaff-Weglikowska, U. *Carbon* **2004**, *42*, 1159–1164.
23. Klemm, D.; Schumann, D.; Udhardt, U.; Marsch, S. *Prog. Polym. Sci.* **2001**, *26*, 1561–1603.
24. Goyanes, S.; Rubiolo, G. R.; Salazar, A.; Jimeno, A.; Corcuera, M. A.; Mondragon, I. *Diamond Relat. Mater.* **2007**, *16*, 412–417.
25. Imai, T.; Sugiyama, J. *Macromolecules* **1998**, *31*, 6275–6279.
26. Yamamoto, H.; Horii, F. *Macromolecules* **1993**, *26*, 1313–1317.
27. Brown, R. M., Jr.; Willison, J. H. M.; Richardson, C. *Proc. Natl. Acad. Sci. U.S.A.* **1976**, *73*, 4565–4569.
28. Ross, P.; Weinhouse, H.; Aloni, Y.; Michaeli, D.; Weinberger-Ohana, P.; Mayer, R. *Nature* **1987**, *325*, 279–281.
29. Tokoh, C.; Takabe, K.; Fujita, M.; Saiki, H. *Cellulose* **1998**, *5*, 249–261.
30. Chen, C.-C.; Chen, C.-F.; Chen, C.-M.; Chuang, F.-T. *Electrochem. Commun.* **2007**, *9*, 159–163.
31. Debzi, E. M.; Chanzy, H.; Sugiyama, J.; Tekely, P.; Excoffier, G. *Macromolecules* **1991**, *24*, 6816–6822.
32. Debzi, E. M.; Marchessault, R. H.; Excoffier, G.; Chanzy, H. *Macromol. Symp.* **1999**, *143*, 243–255.
33. Sugiyama, J.; Persson, J.; Chanzy, H. *Macromolecules* **1991**, *24*, 2461–2466.
34. Marechal, Y.; Chanzy, H. *J. Mol. Struct.* **2000**, *523*, 183–196.
35. Sturcova, A.; His, I.; Apperley, D. C.; Sugiyama, J.; Jarvis, M. C. *Biomacromolecules* **2004**, *5*, 1333–1339.
36. Oh, S. Y.; Yoo, D. I.; Shin, Y.; Kim, H. C. *Carbohydr. Res.* **2005**, *340*, 2376–2391.

37. Akerholm, M.; Hinterstoisser, B.; Salmen, L. *Carbohydr. Res.* **2004**, *339*, 569–578.
38. Kataoka, Y.; Kondo, T. *Macromolecules* **1998**, *31*, 760–764.
39. Watanabe, K.; Tabuchi, M.; Morinaga, Y.; Yoshinaga, F. *Cellulose* **1998**, *5*, 187–200.
40. Atalla, R. H.; VanderHart, D. L. *Science* **1984**, *223*, 283–285.
41. Yamamoto, H.; Horii, F. *Cellulose* **1994**, *1*, 57–66.
42. Kono, H.; Yunoki, S.; Shikano, T.; Fujiwara, M.; Erata, T.; Takai, M. *J. Am. Chem. Soc.* **2002**, *124*, 7056–7511.
43. Wada, M.; Sugiyama, J.; Okano, T. *Mokuzai Gakkaishi* **1995**, *41*, 186–192.
44. Wang, Z.; Ba, D. C.; Liu, F.; Cao, P. J.; Yang, T. Z.; Gu, Y. S.; Gao, H. J. *Vacuum* **2005**, *77*, 139–144.
45. Uhlin, K. I.; Atalla, R. H.; Thompson, N. S. *Cellulose* **1995**, *2*, 129–144.